ChemComm

COMMUNICATION

View Article Online
View Journal | View Issue

Cite this: *Chem. Commun.*, 2020, **56**, 4015

Received 23rd December 2019,
Accepted 5th March 2020

DOI: 10.1039/c9cc09948d

rsc.li/chemcomm

The elucidation of phospholipid bilayer–small molecule interactions using a combination of phospholipid nanodiscs and solution state NMR techniques†

Georgina Townshend,[ab] Gary S. Thompson,[b] Lisa J. White,[a] Jennifer R. Hiscock *[b] and Jose L. Ortega-Roldan*[a]

Quantifying phospholipid bilayer–small molecule interactions is vital to the development of new drug candidates and/or medicinal therapies. However, obtaining these data remains problematic. Herein, we detail a phospholipid nanodisc assay which enables the elucidation of these interactions using conventional solution state NMR spectroscopy techniques.

The quantification of small molecule–phospholipid bilayer interactions is inherently difficult but is incredibly important for the development of novel pharmaceuticals,[1] drug delivery systems,[2] synthetic membrane transporters[3] and ion channel technologies.[4] Although a variety of methodologies exist to study these interactions,[5] the most common of these centre around the use of synthetic vesicles combined with fluorescence spectroscopy. For example, vesical leakage assays allow the identification of membrane disruption, which results in the release of a self-quenching fluorescent cargo.[6] The use of fluorescence anisotropy allows the calculation of small molecule–membrane association constants[7] and observation of membrane fluidity.[8] However, incorporating a fluorescent unit within an experiment is not always possible for either synthetic or financial reasons. In addition, the presence of fluorescent reporter units may also enhance or suppress the response being monitored leading to erroneous results. Limitations also exist in relation to the synthetic vesicle cell membrane mimic: (i) the enhanced membrane curvature exhibited in vesicles has been shown to influence molecule:membrane binding and/or insertion events;[9] (ii) synthetic vesicles, commonly produced *via* extrusion through porous filters can, often unknowingly, result in the production of unwanted multilamellar, alongside the desired unilamellar structures.[10]

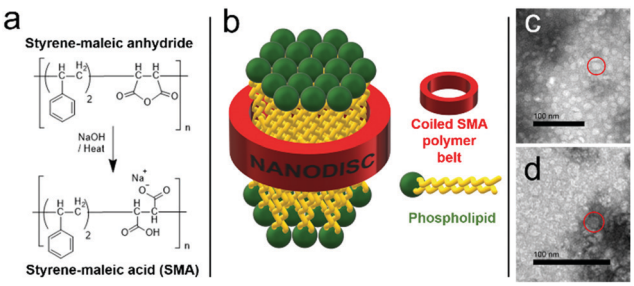

Fig. 1 (a) Reaction scheme detailing the production of the SMA belt; (b) cartoon of a SMA belted phospholipid nanodisc; (c and d) TEM images of dehydrated SMA nanodiscs, stained with uranyl acetate, formed from (c) DMPC phospholipids and (d) *E. coli* phospholipids. Red circles indicate a single ≈10 nm nanodisc.

In recent times, innovative solid-state NMR techniques have been developed to study molecule–membrane interactions,[11] however access to these specialised methodologies remains difficult. In this study, we demonstrate the use of phospholipid nanodiscs (Fig. 1) in a novel yet accessible, high throughput NMR assay to allow the quantification of small molecule: phospholipid interactions, removing the limitations detailed previously.

Traditionally phospholipid nanodiscs have been used to enable the study of membrane proteins however, the potential for nanodiscs to quantify synthetic compound–membrane interactions remains underdeveloped.[12] These biomimetic scaffolds are composed of a single disc-shaped planar phospholipid bilayer, 'belted' with membrane scaffolding proteins or synthetic polymers. Examples include amphipathic peptides[13] such as Saposin-A[14] and, synthetic molecules such as styrene-maleic acid (SMA) co-polymers.[15] Unlike alternative membrane mimetic systems, nanodiscs have been shown to maintain many desirable physical properties of the membrane bilayer such as lipid phase transition temperatures and lipid bilayer thickness.[16] Although the peptide-based nanodiscs typically require solubilisation in detergent prior to formation, with the lipid : protein : detergent ratios optimised for each lipid mixture, SMAs are able to solubilise

[a] *School of Biosciences, University of Kent, Canterbury, Kent, CT2 7NJ, UK. E-mail: J.L.Ortega-Roldan@kent.ac.uk; Tel: +44 (0)1227 824730*

[b] *School of Physical Sciences, University of Kent, Canterbury, Kent, CT2 7NH, UK. E-mail: J.R.Hiscock@Kent.ac.uk; Tel: +44 (0)1227 823043*

† Electronic supplementary information (ESI) available: This includes experimental details, nanodiscs synthesis and quantification, DLS, zeta potential, TEM, NMR spectroscopy data. See DOI: 10.1039/c9cc09948d

natural lipid membranes of any composition, forming nanodiscs with an average diameter of 10 nm, without the presence of detergent.[16]

For this proof of principle study, SMA with a ratio of 2 : 1 styrene to maleic acid (Fig. 1a) was incubated with either bacterial (*Escherichia coli* (*E. coli*), lipid composition = 67% Phosphatidylethanolamine – PE, 23.2% phosphatidylglycerol – PG and 9.8% cardiolipin) or 1,2-dimyristoyl-*sn*-glycero-3-phosphocholine (DMPC) phospholipid vesicles. The nanodiscs formed (Fig. 1c and d) were then separated from the resultant mixture through a combination of ultracentrifugation and gel filtration (ESI†).

Quantification of nanodisc concentration was achieved utilizing the absorbance of the free SMA at 260 nm. These absorbance values were found to follow a linear trend with concentration, discarding any association of the SMAs at higher concentrations >165 μM. It is known that a single SMA is used to 'belt' a single $\approx$10 nm nanodisc.[16]

Compounds **1–3**[17] (Fig. 2) are representatives from a novel class of supramolecular self-associating amphiphile (SSA),[18] members of which have been shown to act as antimicrobial agents.[19] The amphiphilic nature of SSAs, combined with the mixture of hydrogen bond donating and accepting groups within the molecular scaffold has led us to hypothesise that SSAs may act as bacterial membrane disrupters. Further to this, we believe that this class of compound may be tuned to interact selectively with phospholipids more commonly found at the exterior bacterial (PE and PG)[20] over eukaryotic (phosphatidylcholine – PC)[21] cell membrane, through optimisation of complimentary SSA–phospholipid head group interactions (Fig. 3).

We have shown SSAs to undergo complex self-association events in aqueous conditions, leading to the production of spherical aggregates with a hydrodynamic diameter of $\approx$150–250 nm. The Critical Micelle Concentration (CMC) of **1–3** in a H_2O : EtOH 19 : 1 solution has previously been determined (**1** = 9.54 mM,[17a] **2** = 0.50 mM,[17a] and **3** = 10.39 mM[18a]). All nanodisc association experiments were performed at a SSA concentration of 0.10 mM, at least five times lower than the lowest SSA CMC value reported, therefore the majority of the SSA in solution will exist as monomeric or lower order self-associated species, observable *via* conventional solution state NMR techniques. However, the size of the SMA nanodiscs ($\approx$10 nm in diameter) means these structures cannot be readily observed using analogous techniques. The 1D ^{1}H NMR spectra

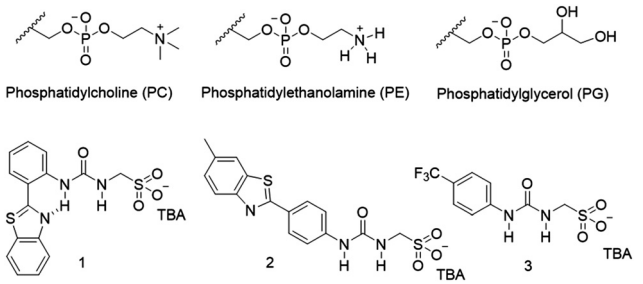

Fig. 2 Structure of phospholipid head groups and SSAs **1–3**. TBA = tetrabutylammonium.

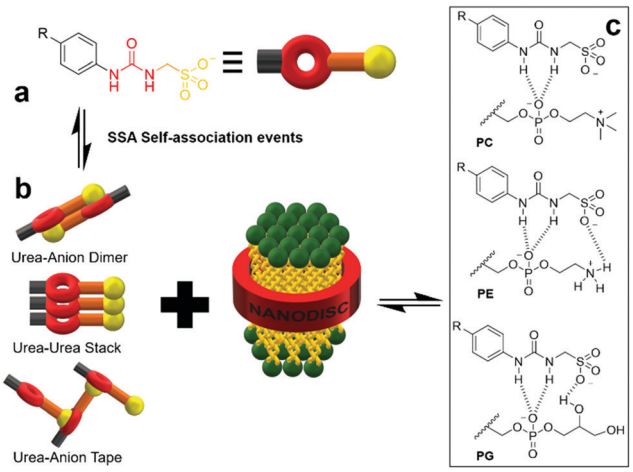

Fig. 3 Scheme showing: (a) a representative structure of the anionic SSA component; (b) hydrogen bonded self-associative events observed for the anionic components of SSAs in the solid state;[18c] (c) hypothesised hydrogen bonding interactions of the anionic component of a SSA with different phospholipid head groups.

of the SMA nanodiscs are broad and include resonances from 0.7 to 8.0 ppm. For this reason, the well separated aromatic ^{1}H NMR resonances of **1–3** (Fig. S11–S34, ESI†) were chosen to monitor the nanodisc:SSA anion association events. The nanodisc:SSA cation association events were monitored simultaneously, through the observation of the ^{1}H NMR tetrabutylammonium (TBA) ion signals (0.8 to 3.3 ppm). During these association experiments the SSAs were maintained at a fixed concentration (0.1 mM), to remove any additional SSA interaction events which are not the result of increasing nanodisc concentration. The association of SSAs to the nanodiscs was then observed using 1D ^{1}H NMR with a Carr–Purcell–Meiboom–Gill sequence (CPMG) filter (300 ms),[22] through comparative integration, as illustrated in Fig. 4. The use of a CPMG filter suppresses the resonances of those species with long correlation times and is therefore very sensitive to the interaction of small chemical compounds to the comparatively large nanodisc structures.

The results of these SSA anion:nanodisc complexation studies are summarised in Fig. 5, 6 and Fig. S35 and S36 (ESI†). Compound **2** was the only SSA of those tested to show full suppression of the SSA anion signal in the presence of *E. coli* phospholipid nanodiscs (Fig. 5a), indicating the high affinity of this SSA anion for the nanodisc. The affinity of this same SSA anion to DMPC nanodiscs was also shown to be significantly lower, with the comparative decrease in signal area plateauing at >2 times higher SSA : nanodisc ratios than those observed in the presence of *E. coli* lipids.

In comparison, the anionic components of **1** and **3** show a similar affinity for both DMPC and *E. coli* nanodiscs (Fig. S35 and S36 respectively, ESI†). However, when comparing the chemical structures of **1** and **2**, although both contain a benzothiazole unit appended to the main SSA scaffold, **2** is substituted at the *para* whereas **1** is substituted at the *ortho* position of the analogous benzene ring. The movement of this

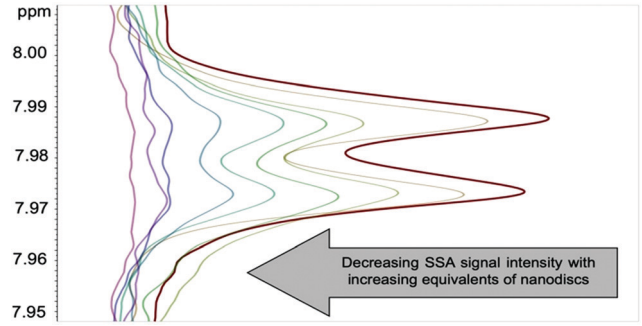

Fig. 4 1D ^{1}H CPMG NMR spectra of **2** (0.10 mM) in the presence of 0.000 (red), 0.002, 0.004, 0.006, 0.008, 0.010, 0.015, 0.021 and 0.032 (purple) molar equivalents of nanodiscs composed of DMPC lipids resulting in decreased signal intensity. 1D ^{1}H CPMG NMR experiments were performed in sodium phosphate buffer (20 mM) with 20 mM sodium chloride at pH 7.4, supplemented with 5% D_2O and 0.01 mM DSS.

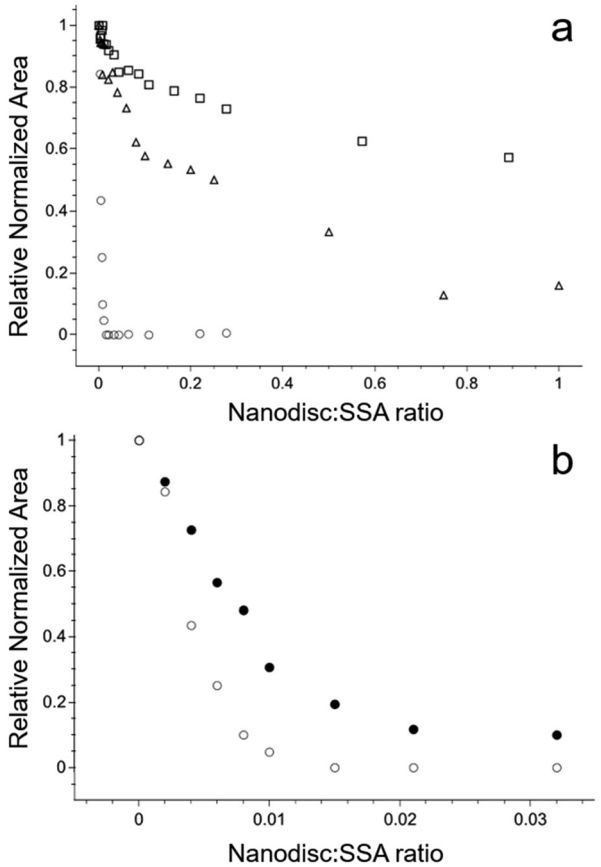

Fig. 5 The relative normalized area of the most downfield aromatic resonance from the SSA anion for: (a) **1** (triangles), **2** (circles), **3** (squares) upon titration with *E. coli* lipid nanodiscs (open symbols); (b) saturation curves for titrations of **2** with *E. coli* lipid (open symbols) and DMPC (filled symbols) nanodiscs.

functionality from the *para* to the *ortho* position results in the formation of an intramolecular hydrogen bond (Fig. 2) which hinders the associative properties of **1** in comparison to **2**.[17a] Therefore, we hypothesise that the presence of the intramolecular hydrogen bond within the structure of **1** results in

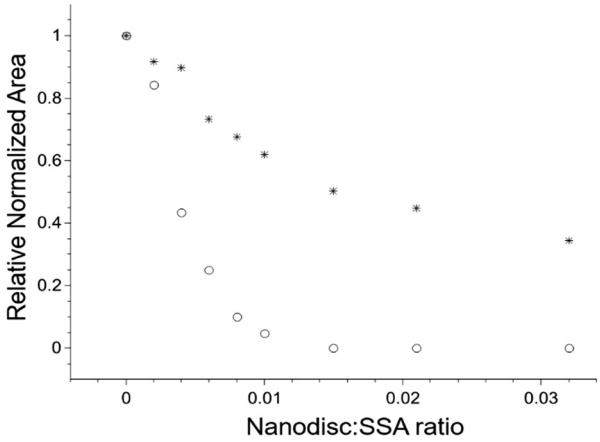

Fig. 6 The relative normalized area of the most downfield resonance from the anionic SSA **2** (open circles) and associated TBA cation (stars) upon titration with *E. coli* nanodiscs.

the decrease of both SSA affinity and selectivity towards nanodisc coordination.

Additionally, the substitution of the benzothiazole unit for the lipophilic, electron withdrawing CF_3 functionality of **3** (Fig. S36, ESI†) is found to further lower the affinity and selectivity of the SSA anion to both *E. coli* lipid and DMPC nanodiscs when compared to **1** and **2**. This is a surprising result, unearthed using this novel assay, which suggests that the *para*-substituted benzothiazole group in combination with the sulfonate-urea functionality, is responsible for both the strength and selectivity of SSA membrane interaction.

Finally, through comparison of those signals that correspond to both the anionic and cationic components of SSAs **1–3**, we have been able to confirm differences in the association of the SSA salt components to the nanodiscs. In the case of SSAs **1** and **3**, the cationic component of the SSA shows greater association to the nanodiscs then the anionic component (Fig. S37–S42, ESI†). However, this observation is reversed for **2**, where the anionic SSA component preferentially interacts with the nanodiscs over the cationic SSA component, as illustrated in Fig. 6.

Although a more detailed thermodynamic analysis of SSA:phospholipid interactions is not yet possible due to: (1) the complex self-associative equilibria observed for SSAs which competes with the SSA:phospholipid complexation processes; (2) the lack of information regarding the reversibility of the lipid association process; (3) the presence of both mass filtering effects and the possible presence of chemical exchange broadening; (4) and, the unknown SSA:nanodisc stoichiometry. The results of these studies do enable the comparative ranking of phospholipid:SSA interactions in the order **2** > **1** > **3** (Fig. 5a), with **2** also showing significant selectivity for bacterial over model eukaryotic DMPC containing nanodiscs.

In summary, the methodology described here allows the analysis of 1D ^{1}H NMR titration data with the aim to enable quantification of small molecule:phospholipid membrane interactions without the need for specialised equipment, or the

experimental limitations commonly encountered through the use of fluorescence based synthetic vesicle studies in the absence of complex equilibria. When complex equilibria are present this proof-of-principle study demonstrates the use of this NMR-based methodology to comparatively rank molecular:nanodisc interactions, resulting in the elucidation of molecular–membrane coordination selectivity and/or specificity. Therefore, although SSA systems are highly complex, demonstrating self-associative interactions in equilibria with SSA:phospholipid nanodisc complex formation, these preliminary results verify the potential for this SSA technology to produce selective cell membrane coordination/disruption systems. We are currently expanding the use of the NMR nanodisc assay described herein to rank the interactions of our current SSA library (>50 compounds) with a wider variety of nanodiscs to inform next generation SSA design. In addition, we are also exploring the importance of SSA cation–anion combinations and presence of the benzothiazole unit within the SSA scaffold to develop ever more selective membrane coordination technologies.

The authors would like to acknowledge the following individuals for their assistance with this work: Dr Timothy Knowles (University of Birmingham); Ian Brown (University of Kent); Dr Arnout Kalverda (University of Leeds); Dr George Williams (University of Kent); and Dr Mark Howard (University of Leeds formally University of Kent). JOR would like to thank the Wellcome Trust for seed award funding (207743/Z/17/Z).

Conflicts of interest

There are no conflicts to declare.

Notes and references

1 (*a*) J. K. Seydel, E. A. Coats, H. P. Cordes and M. Wiese, *Arch. Pharm.*, 1994, **327**, 601–610; (*b*) A. C. Alves, D. Ribeiro, C. Nunes and S. Reis, *Biochim. Biophys. Acta, Biomembr.*, 2016, **1858**, 2231–2244; (*c*) M. Lucio, J. Lima and S. Reis, *Curr. Med. Chem.*, 2010, **17**, 1795–1809; (*d*) E. D. Brown and G. D. Wright, *Nature*, 2016, **529**, 336–343; (*e*) M. A. Sani and F. Separovic, *Acc. Chem. Res.*, 2016, **49**, 1130–1138.

2 (*a*) Y. Li, X. R. Zhang and D. P. Cao, *Nanoscale*, 2015, **7**, 2758–2769; (*b*) E. Blanco, H. Shen and M. Ferrari, *Nat. Biotechnol.*, 2015, **33**, 941–951; (*c*) N. Habibi, N. Kamaly, A. Memic and H. Shafiee, *Nano Today*, 2016, **11**, 41–60.

3 (*a*) G. Y. Jiang, J. G. Wang, Y. Yang, G. X. Zhang, Y. L. Liu, H. Lin, G. L. Zhang, Y. D. Li and X. L. Fan, *Biosens. Bioelectron.*, 2016, **85**, 62–67; (*b*) N. L. Mora, A. Bahreman, H. Valkenier, H. Y. Li, T. H. Sharp, D. N. Sheppard, A. P. Davis and A. Kros, *Chem. Sci.*, 2016, **7**, 1768–1772; (*c*) X. Wu and P. A. Gale, *J. Am. Chem. Soc.*, 2016, **138**, 16508–16514; (*d*) X. Wu, E. N. W. Howe and P. A. Gale, *Acc. Chem. Res.*, 2018, **51**, 1870–1879.

4 (*a*) S. J. Chen, Y. L. Zhao, C. Y. Bao, Y. W. Zhou, C. X. Wang, Q. N. Lin and L. Y. Zhu, *Chem. Commun.*, 2018, **54**, 1249–1252; (*b*) X. Wu, P. Wang, P. Turner, W. Lewis, O. Catal, D. S. Thomas and P. A. Gale, *Chem*, 2019, **5**, 1210–1222; (*c*) K. Gopfrich, C. Y. Li, I. Mames, S. P. Bhamidimarri, M. Ricci, J. Yoo, A. Mames, A. Ohmann, M. Winterhalter, E. Stulz, A. Aksimentiev and U. F. Keyser, *Nano Lett.*, 2016, **16**, 4665–4669; (*d*) W. Si, P. Y. Xin, Z. T. Li and J. L. Hou, *Acc. Chem. Res.*, 2015, **48**, 1612–1619; (*e*) M. Zhang, P. P. Zhu, P. Y. Xin, W. Si, Z. T. Li and J. L. Hou, *Angew. Chem., Int. Ed.*, 2017, **56**, 2999–3003.

5 J. Knobloch, D. K. Suhendro, J. L. Zieleniecki, J. G. Shapter and I. Koper, *Saudi J. Biol. Sci.*, 2015, **22**, 714–718.

6 S. Fiedler and H. Heerklotz, *Biophys.*, 2015, **109**, 2079–2089.

7 (*a*) H. R. Zhang, Q. Wu and M. Y. Berezin, *Expert Opin. Drug Discovery*, 2015, **10**, 1145–1161; (*b*) H. Bensikaddour, K. Snoussi, L. Lins, F. Van Bambeke, P. M. Tulkens, R. Brasseur, E. Goormaghtigh and M. P. Mingeot-Leclercq, *Biochim. Biophys. Acta, Biomembr.*, 2008, **1778**, 2535–2543.

8 B. M. Stott, M. P. Vu, C. O. McLemore, M. S. Lund, E. Gibbons, T. J. Brueseke, H. A. Wilson-Ashworth and J. D. Bell, *J. Lipid Res.*, 2008, **49**, 1202–1215.

9 (*a*) R. Chen and A. E. Mark, *Eur. Biophys. J.*, 2011, **40**, 545–553; (*b*) M. B. Jensen, V. K. Bhatia, C. C. Jao, J. E. Rasmussen, S. L. Pedersen, K. J. Jensen, R. Langen and D. Stamou, *J. Biol. Chem.*, 2011, **286**, 42603–42614.

10 H. L. Scott, A. Skinkle, E. G. Kelley, M. N. Waxham, I. Levental and F. A. Heberle, *Biophys. J.*, 2019, **117**, 1381–1386.

11 J. Medeiros-Silva, S. Jekhmane, A. L. Paioni, K. Gawarecka, M. Baldus, E. Swiezewska, E. Breukink and M. Weingarth, *Nat. Commun.*, 2018, **9**, 3963.

12 A. H. Zhang, I. A. Edwards, B. P. Mishra, G. Sharma, M. D. Healy, A. Elliott, M. A. T. Blaskovich, M. A. Cooper, B. M. Collins, X. Y. Jia and M. Mobli, *Front. Chem.*, 2019, **7**, 238.

13 T. K. Ritchie, Y. V. Grinkova, T. H. Bayburt, I. G. Denisov, J. K. Zolnerciks, W. M. Atkins and S. G. Sligar, *Methods in Enzymology; Liposomes, Pt F*, ed. N. Duzgunes, 2009, vol. 464, pp. 211–231.

14 J. Frauenfeld, R. Loving, J. P. Armache, A. F. P. Sonnen, F. Guettou, P. Moberg, L. Zhu, C. Jegerschold, A. Flayhan, J. A. G. Briggs, H. Garoff, C. Low, Y. F. Cheng and P. Nordlund, *Nat. Methods*, 2016, **13**, 345–351.

15 S. C. Lee, T. J. Knowles, V. L. G. Postis, M. Jamshad, R. A. Parslow, Y. P. Lin, A. Goldman, P. Sridhar, M. Overduin, S. P. Muench and T. R. Dafforn, *Nat. Protoc.*, 2016, **11**, 1149–1162.

16 M. Jamshad, V. Grimard, I. Idini, T. J. Knowles, M. R. Dowle, N. Schofield, P. Sridhar, Y. P. Lin, R. Finka, M. Wheatley, O. R. T. Thomas, R. E. Palmer, M. Overduin, C. Govaerts, J. M. Ruysschaert, K. J. Edler and T. R. Dafforn, *Nano Res.*, 2015, **8**, 774–789.

17 (*a*) L. J. White, N. J. Wells, L. R. Blackholly, H. J. Shepherd, B. Wilson, G. P. Bustone, T. J. Runacres and J. R. Hiscock, *Chem. Sci.*, 2017, **8**, 7620–7630; (*b*) J. R. Hiscock, G. P. Bustone, B. Wilson, K. E. Belsey and L. R. Blackholly, *Soft Matter*, 2016, **12**, 4221–4228.

18 (*a*) L. J. White, S. N. Tyuleva, B. Wilson, H. J. Shepherd, K. K. L. Ng, S. J. Holder, E. R. Clark and J. R. Hiscock, *Chem. – Eur. J.*, 2018, **24**, 7761–7773; (*b*) T. L. Gumbs, L. J. White, N. J. Wells, H. J. Shepherd and J. R. Hiscock, *Supramol. Chem.*, 2018, **30**, 286–295; (*c*) L. R. Blackholly, H. J. Shepherd and J. R. Hiscock, *CrystEngComm*, 2016, **18**, 7021–7028.

19 S. N. Tyuleva, N. Allen, L. J. White, A. Pepes, H. J. Shepherd, P. J. Saines, R. J. Ellaby, D. P. Mulvihill and J. R. Hiscock, *Chem. Commun.*, 2019, **55**, 95–98.

20 C. Sohlenkamp and O. Geiger, *FEMS Microbiol. Rev.*, 2016, **40**, 133–159.

21 G. V. Meer and A. I. P. M. D. Kroon, *J. Cell Sci.*, 2011, **124**, 5–8.

22 (*a*) S. Meiboom and D. Gill, *Rev. Sci. Instrum.*, 1958, **29**, 688–691; (*b*) H. Y. Carr and E. M. Purcell, *Phys. Rev.*, 1954, **94**, 630–638.

